



OPEN The neurotoxicity of Paraquat and its degradation products on *Drosophila melanogaster*

Douglas Lisboa Ramalho¹, Jadyellen Rondon Silva^{1,2},
 Maria Eduarda Monteiro Martins dos Santos^{1,3}, Maria Eduarda Silva Soares^{1,4},
 Andrielle Adelina Teodoro Jesus^{1,4}, Thiago Henrique Oliveira Alves^{1,4},
 Michelle Fernanda Brugnera⁵, Sidnei Moura⁶ & Anderson Oliveira Souza^{1,2,3,4}✉

Photodegradation is a promising technique for remediating contaminated environmental matrices. It demonstrates significant potential in transforming organic contaminants into carbon dioxide, water, and inorganic anions through degradation reactions that involve transient oxidizing species, mainly hydroxyl radicals generated by ultraviolet (UV) irradiation. In this study, we investigated whether the photodegradation of Paraquat (PQ) with UV irradiation reduced its toxicity in *Drosophila melanogaster*. Our results indicate that ingesting PQ degradation products by larvae resulted in a low axial ratio (pupal volume). In the adults, it resulted in markedly diminished climbing ability in a time-dependent manner after 10 days of feeding. In addition, exposure of *D. melanogaster* to photodegradation of PQ reduced acetylcholinesterase and citrate synthase activities but improved oxidative stress, as evidenced by protein carbonyl, and lactate production. These results suggest that the photodegradation of PQ with UV irradiation produced PQ fragments with higher toxicity than PQ, while the precise mechanism of its action requires further investigation.

Keywords Photodegradation, Degradation products, *Drosophila melanogaster*, UV irradiation, Neurotoxicity

The increase in world population in the 20th century would not have been possible without a parallel growth in food production, and this was achieved with agrochemicals, which are currently important components of the world's agricultural systems¹. Nevertheless, studies show the negative impacts of farming residues on soils and aquatic ecosystems that can have toxic effects on animals and humans².

Paraquat (PQ) is a widely used bipyridyl herbicide whose mode of action is based on the deflection of electrons from photosystem I, producing reactive oxygen species (ROS), and causing cell death in the target organism due to the destruction of fatty acids in the thylakoids and other membranes^{3,4}. PQ has a negligible vapor pressure at room temperature, being practically non-volatile⁵. Additionally, it has a high sorption coefficient (Koc) of 4×10^3 mg/dL, a half-life of approximately six years, and low degradation by microorganisms⁴, guaranteeing adequate bioavailability for roots in the soil. This compound is persistent in the environment causing problems for animals and humans^{5–7}.

Nowadays, PQ is banned in more than 50 countries worldwide, including China, South Korea, the European Union, and the United Kingdom. In other countries such as the United States, Australia, Colombia, Chile, Uruguay, and Japan, paraquat is under re-evaluation and/or strictly controlled use⁸.

Studies have highlighted the toxicity of PQ for animals. The oral mean lethal dose (LD50) varies from 22 to 262 mg/Kg, depending on the species^{9,10}, and there are no antidotes after exposition^{7,10,14}. PQ impairs bioenergetic function, mitochondrial metabolism, and the aggregation of α -synuclein and amyloid precursor protein (APP), crucial proteins involved in neurodegenerative processes^{11–13}. In addition, this compound is

¹Mitochondrial Metabolism and Neurotoxicology Laboratory, Department of Chemistry, Institute of Chemistry, Federal University of Mato Grosso, Cuiabá, Brazil. ²Postgraduate Program in Biodiversity and Biotechnology of the BIONORTE Network (PPG-BIONORTE), Federal University of Mato Grosso, Cuiabá, Brazil. ³Food and Nutrition Department, Federal University of Mato Grosso, Cuiabá, Brazil. ⁴Postgraduate Program in Health Sciences, Federal University of Mato Grosso, Cuiabá, Brazil. ⁵Biocide Residue Analysis Laboratory, Department of Chemistry, Institute of Chemistry, Federal University of Mato Grosso, Cuiabá, Brazil. ⁶Biotechnology of Natural and Synthetic Products Laboratory, Institute of Biotechnology, University of Caxias do Sul, Caxias do Sul, Brazil. ✉email: anderson.souza@ufmt.br

similar to 1-methyl-4-phenyl-1,2,3,6-tetrahydropyridine (MPTP), a dopaminergic neurotoxin widely used as an inducer of Alzheimer’s and Parkinson’s diseases in experimental animal models^{14–18}.

Studies describe that the physicochemical and biological processes are efficient in removing organic environmental contaminants, such as PQ, from water and wastewater^{19–21}. In this context, Advanced Oxidative Processes (AOP) stand out. Among these, photolysis has demonstrated potential for application in the degradation of organic pollutants through UV radiation due to its promise due to its low price, high efficiency, and non-toxic properties^{22–24}. The basis for the use of AOPs for the remediation of organic and inorganic toxins lies in the fundamental reactions of ROS. While kinetic parameters and reaction pathways have been determined for the aqueous-based free-radical-mediated destruction of numerous problematic pollutants, simple organic compounds can involve complex reaction pathways and product mixtures²⁵. The generation of hydroxyl radicals by various homogeneous and heterogeneous AOPs can also affect different reaction dynamics and lead to significantly different reaction pathways that could be more toxic than the original compound.

The study of the toxic effect of chemical compounds such as PQ requires the use of animal models, in this case, the insect *Drosophila melanogaster*, known as the “fruit fly” the closest invertebrate model to humans due to its conserved evolutionary genetics and development biology. This insect has high reproductive capacity, fast development, short lifespan, and conserved biological processes, making it an ideal toxicological assessment model²⁶. In addition, the daily food consumption of a single *D. melanogaster* is approximately 1.5 uL, representing 1.7 times its body mass²⁷, and females in the maturation stage of fertilized eggs consume more solid food than virgin females²⁸.

Toxicological studies targeting residual compounds generated in AOPs, and their ecological impacts²⁹ and insect health are not fully defined. In this work, we present the neurotoxic effects on behavioral, physiological, and biochemical parameters in *D. melanogaster* caused by the photodegradation derivatives of PQ by means of a UV light source. This study can help guide the recommendations for compounds generated in AOPs and their toxic effects.

Materials and methods
Samples

To prepare the aqueous solution fortified with Paraquat, PQ (CAS n. 75365-73-0) 79 mM, final concentration, ultrapure water (18.2 MΩ cm) was used from a water purification system (Q-Gard[®] connected to Elix[®]/RO/distilled water, model QGARD00R1, Merck, USA). The solution was then treated in a photodegradation system for 60 min, and 5 aliquots with 0.18 mL were collected at times 0; 10; 15; 30; and 60 min, and then stored at −20 °C ± 01 °C in a hermetically closed flask, in absence of light, until they are used to supplement standard diets and chemical characterization (0; 10; 15 and 30 min).

The photocatalytic degradation was done using a photoreactor equipped with water cooling through a thermostatic bath (model CE-110/10, Cienlab). In a quartz bulb, the photocatalyst was irradiated with a UV light source (315–400 nm) using a 125 W Philips medium-pressure mercury lamp without the glass²².

Chemical characterization by high-resolution mass spectrometry - HRMS

All samples (PQ; photodegradation of PQ during 15 min and 30 min) were lyophilized and subsequently solubilized in 50% (v/v) chromatographic grade acetonitrile (CAS n. 75-05-8, Tedia, Fairfield, OH, USA), 50% (v/v) deionized water, and 0.1% formic acid (CAS n. 64-18-6) for positive mode ESI(+). The solutions were infused directly into the ESI source using a syringe pump (Harvard Apparatus) at a flow rate of 150 μL/min. ESI(+)-MS and tandem ESI(+)-MS/MS were acquired using a hybrid high-resolution and high accuracy (5 μL/L) microTof (Q-TOF) mass spectrometer (Bruker[®] Scientific) under the following conditions: capillary and cone voltages were set to + 3500 V and + 40 V, respectively, with a de-solvation temperature of 100°C. For ESI(+)-MS/MS, each component’s energy for the collision-induced dissociations (CID) was optimized. Diagnostic ions in different fractions were identified by the comparison of their exact mass (*m/z*), isotopic ratio, and ESI(+)-MS/MS dissociation patterns with compounds identified in previous studies (Table 1). QTOF-control data analysis software (Bruker[®] Scientific) (<https://www.bruker.com>) was used for data acquisition and processing. The data were collected in the *m/z* range of 50–1400 at the speed of two scans per second, providing a resolution of 50,000 (FWHM) at *m/z* 200. No important ions were observed below *m/z* 50 or above *m/z* 850 therefore ESI(+)-MS data is shown in the *m/z* 50 – 850 range.

Entry	Compound	Precursor ion <i>m/z</i>	Formula	Error (ppm)	Isotopic ratio (mSig)	Fragmentation pathway
1	-	93.0601	C ₆ H ₇ N ⁺	-	3.3	-
2	Monoquat	171.0915	C ₁₁ H ₁₁ N ₂ ⁺	4.2	5.3	155.0604 [M – CH ₄] ⁺ ; 143.0728 [M – CH ₃ N] ⁺ ; 128.0499 [M – C ₂ H ₅ N] ⁺ ; 115.0544 [M – C ₂ H ₄ N] ⁺ ; 103.0521 [M – C ₃ H ₄ N ₂] ⁺
3	Paraquat	185.1073	C ₁₂ H ₁₃ N ₂ ⁺	3.0	2.1	171.0911 [M – CH ₂] ₂ ⁺ ; 158.0962 [M – CHN] ₂ ⁺ ; 144.0807 [M – C ₂ H ₃ N] ₂ ⁺ ; 118.0656 [M – C ₄ H ₅ N] ₂ ⁺ ; 107.0738 [M – C ₅ H ₄ N] ₂ ⁺
4	-	300.1608	C ₂₁ H ₂₀ N ₂ ⁺	6.0	4.5	

Table 1. ESI(+)-MS/MS dissociation patterns.

Fly strain and rearing

All experiments in this study were performed using *Canton Special* (wild strain) flies. The flies were cultured at 25 ± 1 °C on a standard diet containing cornmeal (6.5% m/v), agar (CAS n. 9002-18-00) (1.0% m/v), yeast (6.5%) and Nipagin (CAS n. 99-76-3) (3.0% v/v)³⁰.

Exposure of photodegradation samples to *Drosophila melanogaster*

Flies (male and female) were maintained in three different experimental conditions for 3 h, the eggs deposited for 3 h were hatched, and the larvae were fed: (1) A standard diet containing cornmeal (6.5% m/v), agar (CAS n. 9002-18-00) (1.0% m/v), yeast (6.5%) and Nipagin (CAS n. 99-76-3) (3.0% v/v)³⁰; (2) A standard diet supplemented with a solution of PQ 0.474 mM (final concentration) and (3) A standard diet was supplemented with 180 µL of aliquots by photodegradation of PQ during 10 min. The aliquots were selected based on a preliminary toxicity assessment.

All female thoraces (50 samples/Eppendorf) and heads (50 samples/Eppendorf) after 10 days of treatment were dissected and homogenized with tungsten carbide beads (cat no 69997, Qiagen) in a solution (NaCl 0.9%, pH 7.0) (CAS n. 7647-14-5) containing a protease inhibitor diluted to 1:200 (CAS n. 66701-25-5). The homogenates were centrifuged at 10,000 x g for 10 min at 4°C, posteriorly the supernatant was collected and stored at –20 °C until use.

Determination of the pupal volume of *D. melanogaster*

After five days, the larvae fed different diets, begin the metamorphosis into adult animals. To evaluate the effect of photodegradation of PQ samples on the volume of *D. melanogaster* pupae, we calculated the volume or axial ratio (length/width) of 40 pupae³¹.

Survival assay

The effect of PQ photodegradation products on adult flies' lifespan was studied on newly emerged flies. The flies were transferred to untreated (control) at different times (15 and 30 min) of PQ photodegradation from day one of their emergence (100 flies/vial and 5 vials/group). The flies were transferred to the standard diet and supplemented every 2 days with fresh food maintained for the best physiological conditions and to avoid insect death caused by humid food, mold, or bacterial growth³². Mortality was recorded in each vial for 20 days.

Climbing assay

The locomotor behavior of the flies was measured using a counter-current apparatus³³. The newly emerged flies (2, 5, 10, 15, and 20 days old) were placed in empty cylindrical tubes with a height of 15 cm. The flies were then tapped down to the bottom and allowed 60 s to climb 15 cm from the bottom of the vial. The experiment was performed in five trials/replicates. Results were obtained by phototaxis index $\Sigma(i \cdot Ni)/N$ with N representing the total number of *D. melanogaster* assayed, in the scale number, and Ni number of flies in the tube at the end of the experiment³⁴.

Indirect measurement of oxide nitric (•NO) by the griess reaction

The Griess A solution was adapted from de Vargas-Maya et al. (2021)³⁵ in which 0.1% N-(1-naphthyl) ethylenediamine dihydrochloride (CAS n. 1465-25-4) prepared in Milli-Q water was used. Solution B: 1% sulfanilamide (CAS n. 63-74-1) prepared in 5% phosphoric acid (CAS n. 7664-38-2). For nitrite (CAS n. 7632-00-0) concentrations in the nitrite standard curve ranging from 0.5 to 20 µM, the final concentration was prepared in each experiment by measuring biological samples. The standard curve and analysis of the biological sample were prepared by adding 50 µL of Solution A and 50 µL of Solution B and then added to a 96-well plate. Reactions were incubated at room temperature for 15 min, protected from light. Optical density was measured at 540 nm spectrophotometrically using a spectrophotometer (Model Cary 50MPR Varian Ltd., Melbourne, Australia).

Protein carbonyl

Thoraces and heads of *D. melanogaster* were homogenized in ice-cold 100 mM Tris buffer, pH 7.4, and centrifuged at 1500xg for 10 min at 4°C. Supernatants were separated into two fractions, resuspended with 10% trichloroacetic acid (TCA) (CAS n. 76-03-9), and centrifuged at 5000xg for 10 min at 4°C. One pellet was resuspended in 1 mL 10 mM 2,4-dinitrophenylhydrazine (DNPH) (CAS n. 119-26-6) in 2.5 M HCl (CAS n. 7647-01-0), while the other was resuspended only in 1 mL 2.5 M HCl³⁶. After incubation (1 h, 37 °C, in the dark), samples were transferred to the ice for 10 min, 10% TCA added, and centrifuged at 5000xg for 5 min at 4°C. The pellets were washed three times with 1 mL ethanol (CAS n. 64-17-5)/ethyl acetate (CAS n. 141-78-6) (1:1) and centrifuged at 5000xg for 5 min at 4°C. The pellets were dissolved in 6 M guanidine (CAS n. 50-01-1) and stirred for 40 min. Protein carbonyl content was assessed spectrophotometrically at 340 nm using a Varian Cary 50MPR Spectrophotometer (Varian Ltd., Melbourne, Australia).

Lactate content

Fifty thoraces and heads (dissected and stored at –20 °C in protease inhibitor) were macerated and homogenized in 0.1 M sodium phosphate (CAS n. 7601-54-9) buffer pH 7.4. The homogenate was centrifuged at 10,000xg for 10 min at 4 °C, and the supernatant was collected. Lactate content was measured by the lactate oxidase method, according to manufacturer instructions (Labtest, Brazil, cat. n. #138-1/50). Absorbance was monitored spectrophotometrically at 550 nm using a Varian Cary 50MPR Spectrophotometer (Varian Ltd., Melbourne, Australia). Lactate content was expressed as mg/dL of lactate per total amount of protein in the sample.

Citrate synthase (CS) activity

Fifty thoraces and heads (dissected and stored at -20°C in protease inhibitor) were submitted to homogenization in Tris (200 mM, pH 8.0) with Triton X-100 (CAS n. 9036-19-5) (0.2%v/v)³⁷. Then, the homogenates were centrifuged at $9000\times g$ for 30 min at 4°C , the supernatant was collected, and protein concentration was determined. The CS activity was started by adding 0.01 mg protein to $\sim 170\ \mu\text{L}$ Tris buffer containing 10 mM Acetyl-CoA (CAS n. 32140-51-5), 1 mM 5'-Dithiobis-2-nitrobenzoic acid (DTNB) (CAS n. 69-78-3), and 10 mM oxaloacetate (CAS n. 328-42-7). The reduced CoA (CoA-SH) formed by CS activity converts the DTNB into 2-nitro-5-benzoic acid (TNB). CS activities were evaluated by the rate of TNB formation, measured spectrophotometrically at 412 nm according to Srere (1969)³⁸ using a Varian Cary 50MPR Spectrophotometer (Varian Ltd., Melbourne, Australia).

Acetylcholinesterase (AChE) activity

Fifty thoraces and heads of *D. melanogaster* were homogenized in 100 mM sodium phosphate buffer (containing inhibitor protease), pH 7.4 to disrupt the cells. Homogenates were centrifuged at $9000\times g$ for 30 min at 4°C ¹³. The supernatant (0.01 mg protein) was incubated with 100 mM sodium phosphate buffer, pH 7.4, containing 150 mM acetylthiocholine (CAS n. 1866-15-5) and 1 mM DTNB. AChE activity was determined spectrophotometrically using a Vary Cary 50MPR Spectrophotometer (Varian Ltd., Melbourne, Australia) according to the method of Ellman et al. (1961)³⁹. The results were expressed as nmol conjugated formed/min/mg protein.

Protein assay

The protein concentration was determined by Bradford assay using BSA (CAS n. 9048-46-8) as the standard⁴⁰. The assay consists of the interaction of the protein with the Coomassie Blue reagent (CAS n. 6104-59-2), with the reading carried out at 596 nm.

Statistical analysis

The data are presented as mean \pm S.E.M. N means the number of female flies per group used in each experiment. Statistical analysis was performed using the software GraphPad ©Prism version 7.0 (San Diego, CA, USA) (<https://www.graphpad.com>). The statistical significance of the mean values for multiple comparisons was monitored in control and treated flies using one-way ANOVA with Tukey as post hoc. Results were considered significant when $p < 0.05$ (* $p < 0.05$, ** $p < 0.01$, *** $p < 0.001$, **** $p < 0.0001$) and ns for $p > 0.05$.

Results

Mass analysis and photodegradation

The monitoring of by-products generated in photodegradation processes highlights their ability to transform the vast majority of organic contaminants, such as agrochemicals, into carbon dioxide, water, and inorganic anions^{41,42}. High-resolution mass spectrometry has been applied to qualify and quantify target and non-target compounds isolated and in complex mixtures such as plant extracts⁴³. To confirm the elemental formula, as well as the chemical structure tools such as exact m/z , isotope ratio, and fragmentation profile are used.

Herein, the sample was extracted after 10 min (sample A4) of PQ with UV irradiation. Figure 1 shows the full spectrum for the sample of PQ (A), and 10 min (B) of PQ degradation, where we observe as main m/z 93.0601, 171.0915, 185.1073, and 300.1608, which are related to compounds with $[\text{C}_6\text{H}_7\text{N}]^+$, $[\text{C}_{11}\text{H}_{11}\text{N}_2]^+$, $[\text{C}_{12}\text{H}_{13}\text{N}_2]^+$ and $[\text{C}_{21}\text{H}_2\text{ON}_2]^+$ respectively. Figure 2 demonstrates the presence of the monoquat molecule. In addition, the list of possible intermediate and reaction products is described as supplementary material (Table S1, and S2).

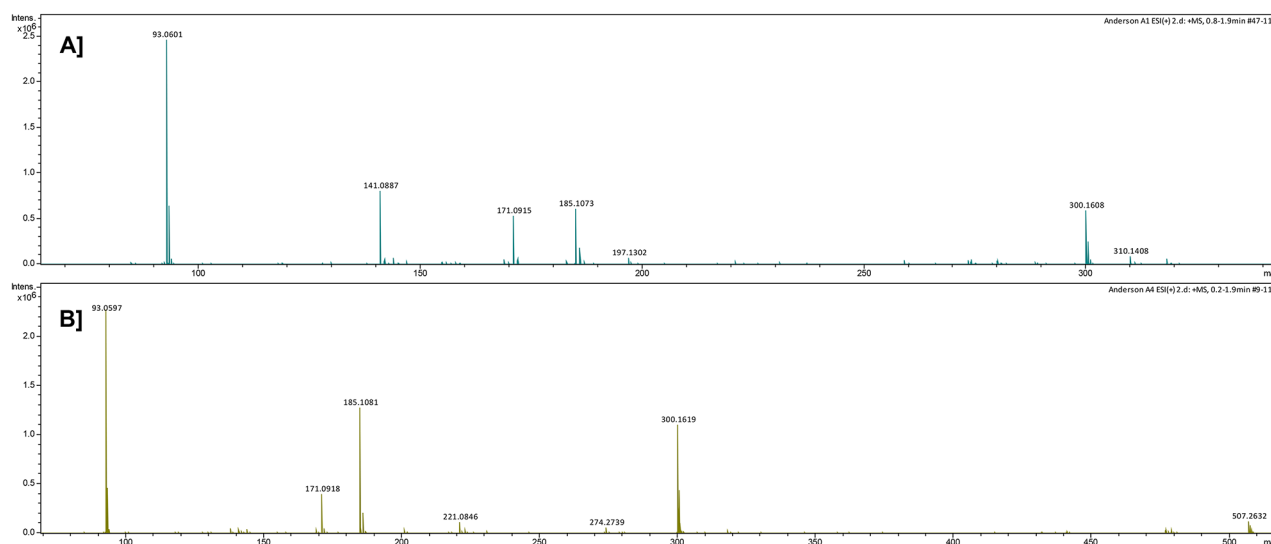


Fig. 1. Full spectra of HRMS for a sample of PQ in (A) and 10 min (B) of PQ with UV irradiation.

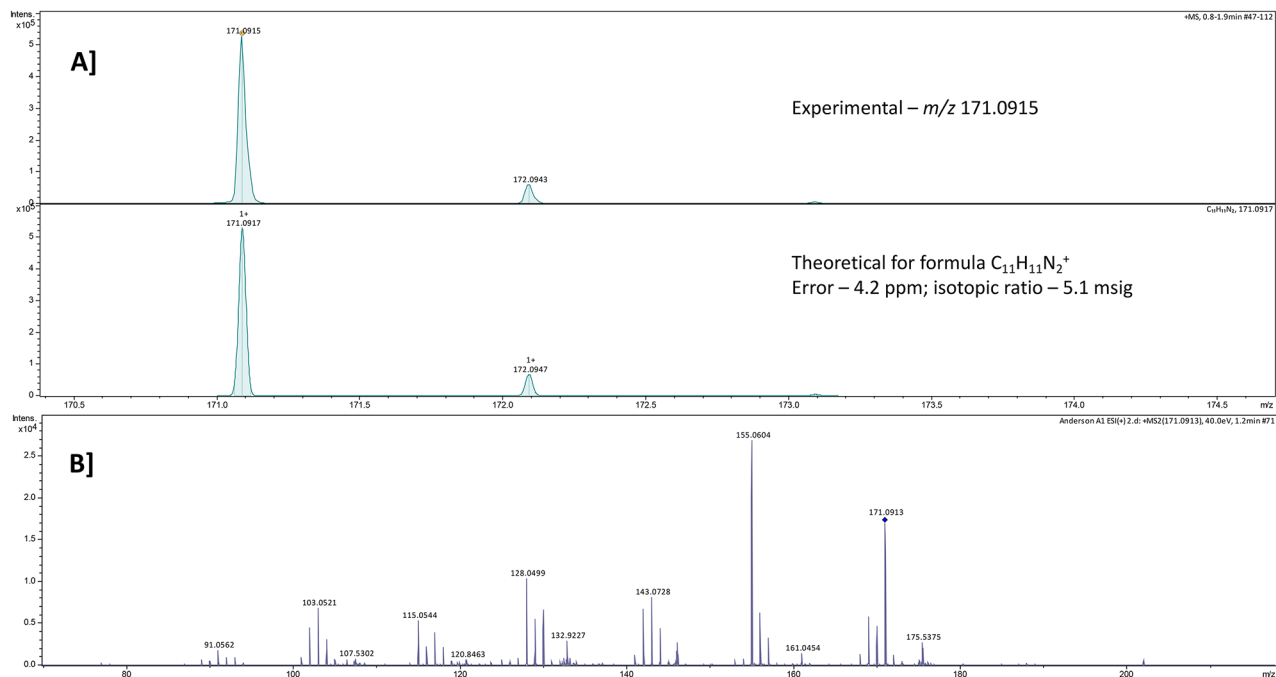


Fig. 2. HRMS for Sample A. In (A) an expansion between 170 and 175 and a comparison with theoretical for the m/z 171.0915; in (B) an analysis in MS-MS mode for the m/z 171.

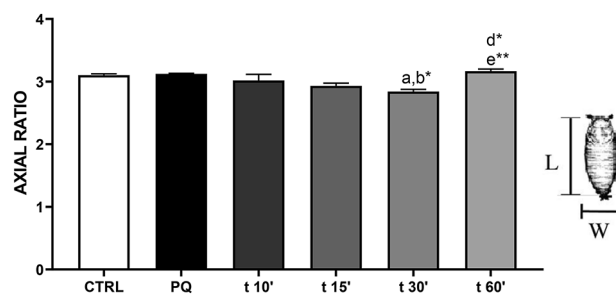


Fig. 3. Quantification of pupal volume in *D. melanogaster* by axial relationship. The body shape of a pupa can be described by length (L) / width (W). The values represent the mean \pm S.E.M of five experiments. The results were considered statistically significant when * $p < 0.05$, ** $p < 0.01$: ^avs. CTRL, ^bvs. PQ, ^cvs. 10 min, ^dvs. 15 min, and ^evs. 30 min of photolysis.

Determination of the pupal volume of *D. melanogaster*

In the development of *D. melanogaster*, the shape, and size at the pupal stage can be conveniently described by the axial ratio of its cuticle (AR, length/width). As shown in Fig. 3, no deleterious effect on the pupal volume was recorded at PQ, however, our results demonstrated a significant reduction in the pupae, whose diets were supplemented with aliquots of 30 min ($p < 0.05$) and 60 min ($p < 0.01$) of photolysis on UV radiation.

Longevity and climbing activity

The PQ and photolysis products added to the semisolid food exerted a significant influence on the fly life span after 10 days (Fig. 4a and Figure S1), with approximately only 97% survival (photolysis for 10 min) compared to 98% in PQ treatment. PQ and products of UV radiation exposure markedly diminished climbing ability in a time-dependent manner (Fig. 4b and Figure S2) after 10 days of feeding.

Indirect measurement of nitric oxide (\bullet NO) by the griess reaction

\bullet NO is a molecule that plays an essential role as a biochemical signal in muscle and neural cells, being an important cofactor in oxidative stress parameters in the body⁴⁴. However, flies fed the fragmentation by-products (Fig. 5a and b) did not show statistical differences from those exposed to PQ degradation by UV irradiation.

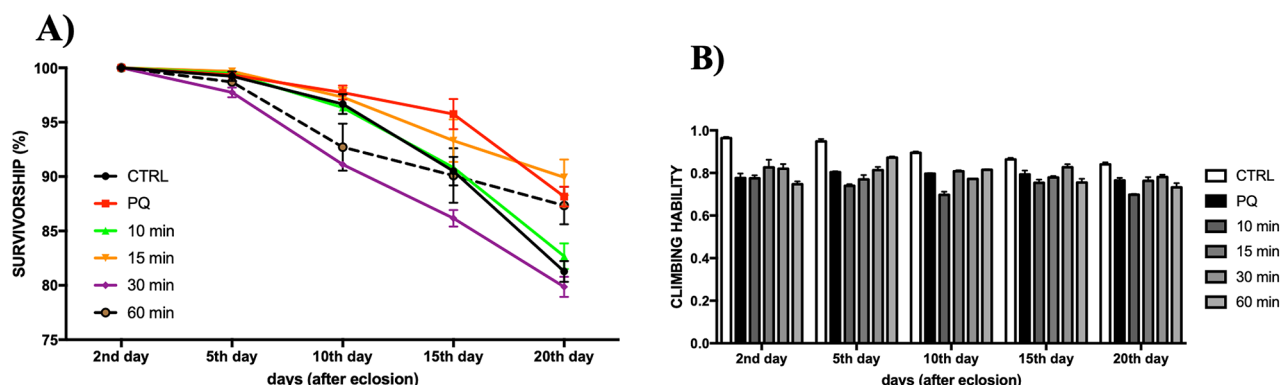


Fig. 4. Behavioral parameters. (A) Lifespan (percentual of survival) of *D. melanogaster* submitted to a diet supplemented with degradation products of PQ and (Figure S1) (B) Climbing ability of *D. melanogaster* fed a diet supplemented with degradation products of PQ and statistical analyses as supplementary material (Figure S2).

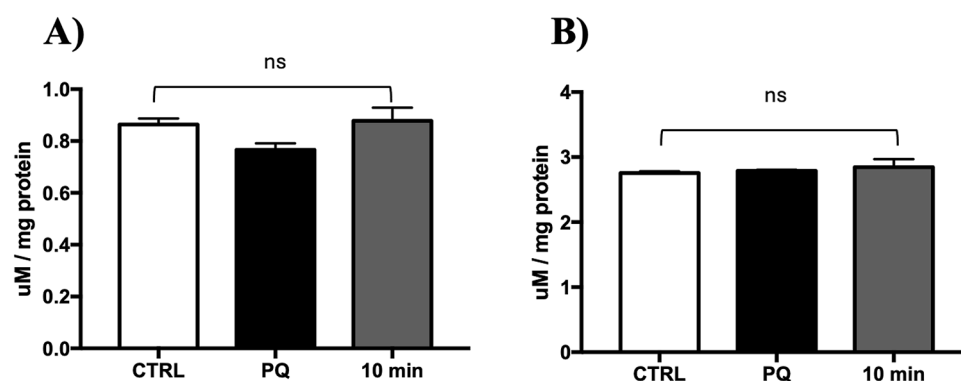


Fig. 5. Indirect measurement of *NO by the Griess Reaction in (A) thoraces and (B) heads of *D. melanogaster* fed on a diet supplemented with PQ and degradation products. The values represent the mean \pm S.E.M of three independent experiments.

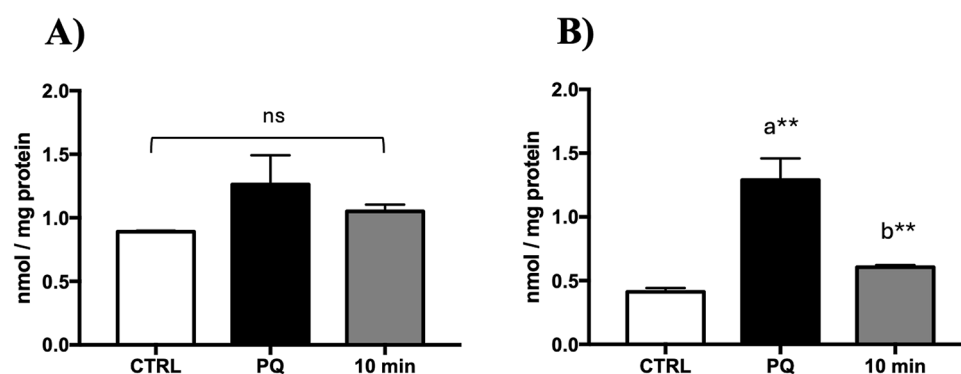


Fig. 6. Protein carbonyl content in (A) thoraces and (B) heads of *D. melanogaster* fed on a diet supplemented with PQ and degradation products. The values represent the mean \pm S.E.M of three independent experiments. The results were considered statistically significant when $^*p < 0.05$, $^{**}p < 0.01$: a vs. CTRL, b vs. PQ.

Protein carbonyl

PQ acts by influencing an intracellular redox cycle inducing an increase in oxidative stress in the intracellular environment¹⁴. Our results demonstrated that flies fed the fragmentation by-products did not show statistical differences from those that fed the PQ degradation by UV irradiation (Fig. 6a). However, there was a significant

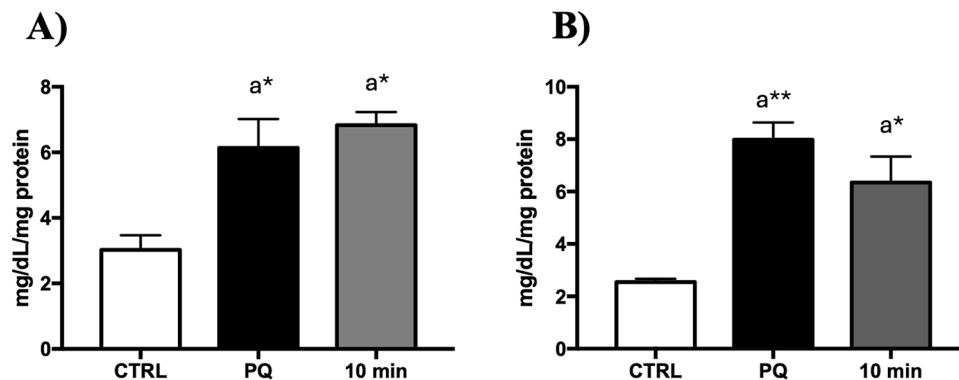


Fig. 7. Lactate concentration in (A) thoraces and (B) heads of *D. melanogaster* fed on a diet supplemented with PQ and degradation products. The values represent the mean \pm S.E.M of three independent experiments. The results were statistically significant when $^*p < 0.05$, $^{**}p < 0.01$: a vs. CTRL.

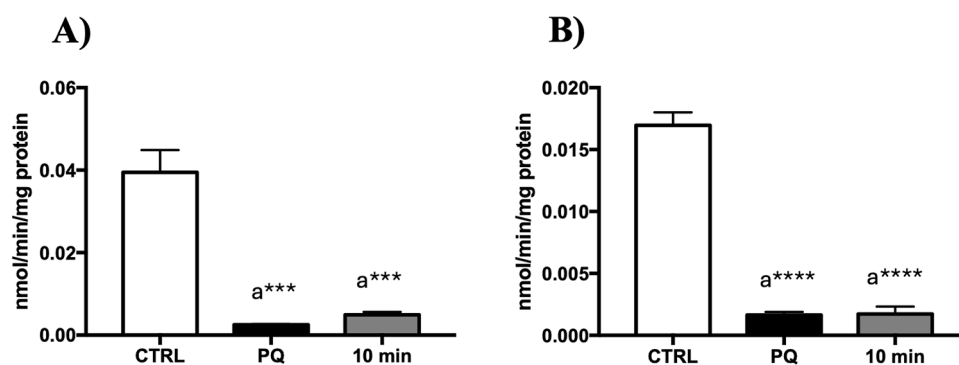


Fig. 8. CS activity in (A) thoraces and (B) heads of *D. melanogaster* fed on a diet supplemented with PQ and degradation products. The values represent the mean \pm S.E.M of three independent experiments. The results were considered statistically significant when $^{***}p < 0.001$, $^{****}p < 0.0001$: a vs. CTRL.

difference in the production of carbonyl proteins as a result of oxidative stress in nervous tissues after exposure to PQ ($p < 0.01$) and 10 min of PQ degradation ($p < 0.01$) (Fig. 6b).

Lactate content

Several studies have demonstrated the importance of lactate dehydrogenase in energy metabolism and as a marker of neuronal oxidative damage that depends on lactate derived from the astrocytes where they are most abundant in the brain⁴⁵. Exposure to PQ ($p < 0.05$) and its photolysis by-products ($p < 0.05$) increased the lactate content in the thoracic muscles (Fig. 7a). In the head, the same effect was shown on the ingestion of PQ ($p < 0.01$) and UV radiation products ($p < 0.05$) (Fig. 7b).

Citrate synthase (CS) activity

Exposure to PQ and its by-products from photolysis reduced the activity of citrate synthase (CS), an enzyme from the Krebs Cycle that indicates mitochondrial content in tissues^{46,47}. However, flies fed with by-products (10 min of fragmentation) showed lower CS activity in the thoracic muscles ($p < 0.001$) (Fig. 8a). In the heads of *D. melanogaster*, the results were significant both in the exposure of PQ and fragments for 10 min of UV radiation ($p < 0.0001$) (Fig. 8b).

Acetylcholinesterase (AChE) activity

AChE activity participates in the cholinergic system, which is involved in the control of acetylcholine (ACh) in the synaptic cleft⁴⁸, being essential in the control of calcium for muscle contraction and various neuronal stimuli^{49,50}. The evaluation of AChE activity demonstrated that diets supplemented with PQ ($p < 0.001$) and its by-products generated by photolysis for 10 min ($p < 0.001$) promoted a significant reduction in AChE activity in the thoracic muscles (Fig. 9a). In the heads of *D. melanogaster*, the results were significant both in the exposure of PQ and fragments for 10 min of UV radiation ($p < 0.0001$) (Fig. 9b).

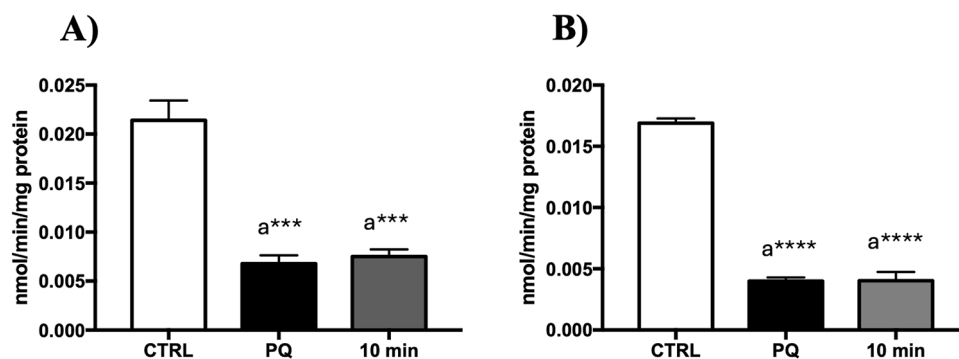


Fig. 9. AChE activity in (A) thoraces and (B) heads of *D. melanogaster* fed on a diet supplemented with PQ and degradation products. The values represent the mean \pm S.E.M of three independent experiments. The results were considered statistically significant when *** p < 0.001, **** p < 0.0001; ^avs. CTRL.

Discussion

In the photolysis of the Paraquat, the pesticide can be degraded by two mechanisms: direct and indirect photolysis. In the case of direct photolysis, the pesticide can absorb energy from UV irradiation, and this energy can cause the molecule to enter an excited state. Degradation can be promoted by homolysis, heterolysis, and photoionization. In indirect photolysis, highly active species, such as hydroxyl, superoxide, and ozone radicals are produced by the excitement of UV light, which can degrade the pesticide⁵¹.

Irradiation with UV light is a potential treatment method for degrading water contaminants, such as natural organic matter, aliphatic and chlorinated volatile organic compounds, aromatic compounds, and herbicides⁵². Herein, the ESI mass spectrum of the PQ solution after photolysis with UV irradiation for 10 min showed the peaks at m/z 300, m/z 186, m/z 171, m/z 138, and m/z 93, studies reported similar detection^{53,54}. However, the ESI mass spectrum of the PQ solution, without irradiation, is mainly characterized by peaks at m/z 186, M^{+} , the molecule ion; m/z 171, ($M^{+}-CH_3$)⁺; m/z 143, ($M^{+}-CH_2NCH_3$)⁺; m/z 118, and m/z 93, M^{2+} , the molecular dication.

The ions at m/z 186, 171, and 93 are the most abundant fragment ions in the PQ solution and PQ fragmentation after a 10 min UV degradation represents the PQ, monoquat, and 4-methyl-pyridine molecules, respectively.

Exposure to PQ in animal models causes drastic damage to bioenergetic function and mitochondrial metabolism^{12,53,54} due to the disturbance of the intracellular redox balance, which promotes an intense cycle of metabolic oxidants⁴⁸, and compromises important aspects in the survival of any animal^{30,46,55}. Our results demonstrated a 5% increase in mortality in animals exposed to fragments generated after 10 min of PQ photolysis. Furthermore, only 2% of flies fed with PQ (0.474 mM, final concentration) for 10 days died, an effect with less toxicity compared to a recent study, which demonstrated the mortality of 20% of *D. melanogaster* fed with 10 mM PQ for 15 days⁵⁶. In addition to its climbing or locomotion capacity, a function directly related to neuromuscular was affected through AChE activity¹³. We observed that by-products generated from the UV radiation are more harmful to the health and survival of the animal model, suggesting greater toxicity to *D. melanogaster*.

PQ may interact with the mitochondrial matrix and with the electron transport chain complexes, especially with complexes I and III promoting a redox cycling: divalent PQ cation (PQ^{2+}) is reduced to highly reactive mono cation radical (PQ^{+}), which in turn reacts with the molecular oxygen to generate superoxide radical ($O_2^{\cdot-}$) and subsequently other oxygen and nitrogen reactive species^{57,58}. Studies reported that a dose of PQ induces oxidative damage that activates mitochondrial pathways associated with excitotoxicity and that autophagy, alteration of dopamine catabolism, and inactivation of tyrosine hydroxylase are mentioned as causes for the loss of dopaminergic cells^{59–62}. Our results showed that PQ solution after photolysis with UV irradiation for 10 min disrupted the intracellular redox balance, promoting an oxidant status, as evidenced by enhanced carbonyl protein production rates in the heads of *D. melanogaster*. In addition, flies exposed to PQ and its photodegradation by-products suffered an increase in the lactate content in the head and thoracic tissues, a key product of energy metabolism in the thorax and brain, catalyzed by the reduction of pyruvate and the accumulation in the brain is a valuable biomarker of neuronal and muscle degeneration related to mitochondrial dysfunction^{45,46,63}.

The diminished mitochondrial metabolism in tissues (muscle and brain) of *D. melanogaster* PQ and its photolysis products supplemented demonstrated here can also be associated with CS activity, an enzyme of Krebs Cycle indicative of mitochondrial content^{47,64}. Flies fed with by-products with 10 min of PQ fragmentation showed lower CS activity in the head and thoracic tissues, suggesting damage to mitochondrial content in neurons. Studies of cell culture^{65,66}, *D. melanogaster*^{13,30,46,67}, and embryos of zebrafish⁶⁸ and mice⁶⁹ PQ-induced mitochondrial dysfunction.

The mechanism of muscle contraction is influenced by several factors including the cholinergic system⁷⁰, with the concentration of ACh being controlled by AChE. PQ and its derivatives, such as monoquat were observed as inhibitors of AChE activity⁷⁰. Our results suggest that the damage to the cholinergic system in flies is due to a significant reduction in AChE, an enzyme whose catalysis favors a greater uptake of calcium for muscle

contraction. In contrast, the central nervous system maintains a balance between neurotransmitters and ACh⁷¹, which shows locomotor impairment in *D. melanogaster*^{72–74}.

Thus, this research offers several contributions to the field, highlighting how our main findings are the significant changes caused by photodegradation of PQ with UV irradiation, with behavioral and biochemical alterations observed in flies. Based on these results, we believe that the toxic effect of PQ fragments is higher when compared to PQ alone.

Conclusion

Flies exposed to PQ suffered significant changes in behavioral and biochemical parameters frequently found in neurodegenerative processes, including reduced climbing activity, mitochondrial dysfunction, cholinergic impairment, and lactate accumulation. In this research, we demonstrated, for the first time, that the photodegradation products of PQ with UV irradiation-induced intoxication in *D. melanogaster* diminished neuromuscular functions such as AChE activity, mitochondrial content, but improved the protein carbonyl levels and lactate content, which reinforces the more toxic effect of PQ fragments when compared to PQ alone. Also, these results are an encouragement for the continuation of this research and further investigations into the possible treatment methods for organic pollutants in wastewater.

Data availability

The datasets generated during and/or analyzed during the current study are available from the corresponding author upon reasonable request.

Received: 6 June 2024; Accepted: 10 January 2025

Published online: 12 May 2025

References

- Geisseler, D. & Scow, K. M. Long-term effects of mineral fertilizers on soil microorganisms – A review. *Soil Biol. Biochem.* **75**, 54–63. <https://doi.org/10.1016/j.soilbio.2014.03.023> (2014).
- Carvalho, F. P. Pesticides, environment, and food safety. *Food Energy Secur.* **6** (2), 48–60. <https://doi.org/10.1002/fes3.108> (2017).
- Bromilow, R. H. Paraquat and sustainable agriculture. *Pest Manag. Sci.* **60** (4), 340–349. <https://doi.org/10.1002/ps.823> (2004).
- Albrecht, A. J. P., Albrecht, L. P. & Silva, A. F. M. Agronomic implications of paraquat ban in Brazil. *Adv. Weed Sci.* **40** (spe1), e020220040–seventy. <https://doi.org/10.51694/AdvWeedSci/2022;40> (2022).
- Sartori, F. & Vidrio, E. Environmental fate and ecotoxicology of paraquat: a California perspective. *Toxicol. Environ. Chem.* **100** (5–7), 479–517. <https://doi.org/10.1080/02772248.2018.1460369> (2018).
- Naito, H. & Yamashita, M. Epidemiology of paraquat in Japan and a new safe formulation of paraquat. *Hum. Toxicol.* **6** (1), 87–88. <https://doi.org/10.1177/096032718700600114> (1987).
- Souza, L. P., Oliveira, J. S. A., Azeredo, T. G. K., Romanholo, R. A. & Vasconcellos, C. Intoxicação Por Paraquat: Dos Cuidados Emergenciais Ao prognóstico. *Revista Científica FAEMA.* **13** (1), 77–91. <https://doi.org/10.31072/rcf.v13i1.922> (2022).
- Albrecht, A. J. P., Albrecht, L. P. & Silva, A. F. M. Agronomic implications of paraquat ban in Brazil. *Adv. Weed Sci.* **40**, 1–13. <https://doi.org/10.51694/AdvWeedSci/2022;40:seventy-five009> (2022).
- Schmitt, G. C. et al. Aspectos gerais e diagnóstico clinicolaboratorial da intoxicação por paraquat. *Jornal Brasileiro De Patologia E Med. Laboratorial.* **42** (4), 235–243. <https://doi.org/10.1590/S1676-24442006000400003> (2006).
- Saravu, K. et al. Paraquat – a deadly poison: report of a case and review. *Indian J. Crit. Care Med.* **17** (3), 182–184. <https://doi.org/10.41103/0972-5229.117074> (2013).
- Chan, H. Y. & Bonini, N. M. *Drosophila* models of human neurodegenerative disease. *Cell Death Differ.* **7** (11), 1075–1080. <https://doi.org/10.1038/sj.cdd.4400757> (2000).
- O’Kane, C. J. *Drosophila* as a Model Organism for the Study of Neuropsychiatric Disorders. (37–60); 10.1007/7854_2010_110 (2011).
- Souza, A. O. et al. Neuroprotective action of Eicosapentaenoic (EPA) and Docosahexaenoic (DHA) acids on Paraquat intoxication in *Drosophila melanogaster*. *NeuroToxicology* **70**, 154–160. <https://doi.org/10.1016/j.neuro.2018.11.013> (2019).
- Baltazar, M. T. et al. Pesticides exposure as etiological factors of Parkinson’s disease and other neurodegenerative diseases - a mechanistic approach. *Toxicol. Lett.* **230** (2), 85–103. <https://doi.org/10.1016/j.toxlet.2014.01.039> (2014).
- Spivey, A. Rotenone and paraquat linked to Parkinson’s Disease: human exposure study supports years of Animal studies. *Environ. Health Perspect.* **119** (6). <https://doi.org/10.1289/ehp.119-a259a> (2011).
- Tanner, C. M. et al. Rotenone, paraquat, and Parkinson’s Disease. *Environ. Health Perspect.* **119** (6), 866–872. <https://doi.org/10.1289/ehp.1002839> (2011).
- Kamel, F. Paths from pesticides to Parkinson’s. *Science* **341** (6147), 722–723. <https://doi.org/10.1126/science.1243619> (2013).
- Thany, S. H., Reynier, P. & Lenaers, G. Neurotoxicité Des pesticides. *Médecine/Sciences* **29** (3), 273–278. <https://doi.org/10.1051/médsci/2013293013> (2013).
- Stefan, M. I. Advanced Oxidation Processes for Water Treatment - fundamentals and Applications. *Water Intell. Online.* **16**, 9781780407197. <https://doi.org/10.2166/9781780407197> (2017).
- Oliveira, D. C. S., Azevedo, P. G. F. & Cavalcanti, L. A. P. Processos biológicos para o tratamento de efluentes: uma revisão integrativa. *Revista Brasileira De Gestão Ambiental E Sustentabilidade.* **8** (18), 397–415. [https://doi.org/10.21438/rbgas\(2021\)081826](https://doi.org/10.21438/rbgas(2021)081826) (2021).
- Alegbeleye, O. et al. Efficient removal of antibiotics from water resources is a public health priority: a critical assessment of the efficacy of some remediation strategies for antibiotics in water. *Environ. Sci. Pollut. Res. Int.* **29** (38), 56948–57020. <https://doi.org/10.1007/s11356-022-21252-4> (2022).
- Brugnera, M. F., Rajeshwar, K., Cardoso, J. C., Zanon, M. V. B. & Bisphenol A removal from wastewater using self-organized TiO₂ nanotubular array electrodes. *Chemosphere* **78** (5), 569–575. <https://doi.org/10.1016/j.chemosphere.2009.10.058> (2010).
- Hossaini, H., Moussavi, G. & Farrokhi, M. The investigation of the LED-activated FeFNS-TiO₂ nanocatalyst for photocatalytic degradation and mineralization of organophosphate pesticides in water. *Water Res.* **59**, 130–144. <https://doi.org/10.1016/j.watres.2014.04.009> (2014).
- Zheng, Z., Zhang, K., Toe, C. Y., Amal, R. & Deletic, A. Photo-electrochemical oxidation flow system for stormwater herbicides removal: operational conditions and energy consumption analysis. *Sci. Total Environ.* **898**, 166375. <https://doi.org/10.1016/j.scitotenv.2023.166375> (2023).
- O’Shea, K. E. & Dionysiou, D. D. Advanced oxidation processes for water treatment. *J. Phys. Chem. Lett.* **3** (15), 2112–2113. <https://doi.org/10.1021/jz300929x> (2012).

26. Pandey, U. B. & Nichols, C. D. Human disease models in *Drosophila melanogaster* and the role of the fly in therapeutic drug discovery. *Pharmacol. Rev.* **63**, 411–436. <https://doi.org/10.1124/pr.110.003293> (2011).
27. Ja, W. W. et al. Prandiology of *Drosophila* and the CAFE assay. *PNAS* **104** (20), 8253–8256. <https://doi.org/10.1073/pnas.0702726104> (2007).
28. Deshpande, S. A. et al. Quantifying *Drosophila* food intake: comparative analysis of current methodology. *Nat. Methods*. **11**, 535–540. <https://doi.org/10.1038/nmeth.2899> (2014).
29. Amondham, W., Parkian, P., Polprasert, C., DeLaune, R. D. & Jugsujinda, A. Paraquat adsorption, degradation, and remobilization in tropical soils of Thailand. *J. Environ. Sci. Health Part. B*. **41**, 485–507. <https://doi.org/10.1080/03601230600701635> (2006).
30. Alencar, L. P. et al. *Piranha trifoliata* extracts ameliorate muscular decline in *Drosophila melanogaster* exposed to Paraquat. *Arch. Insect Biochem. Physiol.* **112** (4). <https://doi.org/10.1002/arch.21994> (2022).
31. Guan, X., Middlebrooks, B. W., Alexander, S. & Wasserman, S. A. Mutation of TweedleD, a member of an unconventional cuticle protein family, alters body shape in *Drosophila*. *Proc. Natl. Acad. Sci.* **103** (45), 16794–16799. <https://doi.org/10.1073/pnas.0607616103> (2006).
32. Bosco, G. et al. Effects of oxygen concentration and pressure on *Drosophila melanogaster*: oxidative stress, mitochondrial activity, and survivorship. *Arch. Insect Biochem. Physiol.* **88** (4), 222–234. <https://doi.org/10.1002/arch.21217> (2015).
33. Simon, A. F. et al. A simple assay to study social behavior in *Drosophila*: measurement of social space within a group. *Genes Brain Behav.* **11** (2), 243–252. <https://doi.org/10.1111/j.1601-183X.2011.00740.x> (2012).
34. Ziegler, A. B. et al. Lack of Dietary Polyunsaturated fatty acids causes synapse dysfunction in the *Drosophila* Visual System. *PLOS ONE*. **10** (8), e0135353. <https://doi.org/10.1371/journal.pone.0135353> (2015).
35. Vargas-Maya, N. I. et al. Refinement of the Griess method for measuring Nitrite in biological samples. *J. Microbiol. Methods*. **187**, 106260. <https://doi.org/10.1016/j.mimet.2021.106260> (2021).
36. Reznick, A. Z. & Packer, L. Oxidative damage to proteins: spectrophotometric method for carbonyl assay (357–363); (1994). [https://doi.org/10.1016/S0076-6879\(94\)33041-7](https://doi.org/10.1016/S0076-6879(94)33041-7)
37. Spinazzi, M., Casarin, A., Pertegato, V., Salviati, L. & Angelini, C. Assessment of mitochondrial respiratory chain enzymatic activities on tissues and cultured cells. *Nat. Protoc.* **7** (6), 1235–1246. <https://doi.org/10.1038/nprot.2012.058> (2012).
38. Srere, P. A. Citrate synthase. *Method Enzymol.* **13**, 3–11. [https://doi.org/10.1016/0076-6879\(69\)13005-0](https://doi.org/10.1016/0076-6879(69)13005-0) (1969).
39. Ellman, G. L., Courtney, K. D., Andres, V. & Featherstone, R. M. A new and rapid colorimetric determination of acetylcholinesterase activity. *Biochem. Pharmacol.* **7** (2), 88–95. [https://doi.org/10.1016/0006-2952\(61\)90145-9](https://doi.org/10.1016/0006-2952(61)90145-9) (1961).
40. Bradford, M. M. A rapid and sensitive method for the quantitation of microgram quantities of protein utilizing the principle of protein-dye binding. *Anal. Biochem.* **72** (1–2), 248–254. [https://doi.org/10.1016/0003-2697\(76\)90527-3](https://doi.org/10.1016/0003-2697(76)90527-3) (1976).
41. Huang, Y., Zhan, H., Bhatt, P. & Chen, S. Paraquat degradation from contaminated environments: current achievements and perspectives. *Front. Microbiol.* **10** <https://doi.org/10.3389/fmicb.2019.01754> (2019).
42. Marien, C. B. D. et al. Kinetics and mechanism of Paraquat's degradation: UV-C photolysis vs UV-C photocatalysis with TiO₂/SiC foams. *J. Hazard. Mater.* **370**, 164–171. <https://doi.org/10.1016/j.jhazmat.2018.06.009> (2019).
43. Pergher, D. et al. Antinociceptive and antioxidant effects of extract enriched with active indole alkaloids from leaves of *Tabernaemontana Catharinensis* A. DC. *J. Ethnopharmacol.* **239**, 111863. <https://doi.org/10.1016/j.jep.2019.111863> (2019).
44. Halliwell, B. & Gutteridge, J. M. C. *Free Radicals in Biology and Medicine* (Oxford University Press, 2015). <https://doi.org/10.1093/acprof:oso/9780198717478.001.0001>
45. Cabral-Costa, J. V. et al. Mitochondrial sodium/calcium exchanger <scp>NCLX regulates glycolysis in astrocytes, impacting on cognitive performance. *J. Neurochem.* **165** (4), 521–535. <https://doi.org/10.1111/jnc.15745> (2023).
46. Silva, M. P. et al. Protective effect of amazonian *Himatanthus sucuba* extracts in *Drosophila melanogaster* exposed to Paraquat. *Res. Soc. Dev.* **11** (17), e148111738931. <https://doi.org/10.33448/rsd-v11i17.38931> (2022).
47. Chhimpia, N., Singh, N., Puri, N. & Kayath, H. P. The Novel role of mitochondrial citrate synthase and citrate in the pathophysiology of Alzheimer's Disease. *J. Alzheimer's Disease*. **94** (s1), S453–S472. <https://doi.org/10.3233/JAD-220514> (2023).
48. Liu, M. & Cholinergics In Encyclopedia of Toxicology (31–34). Elsevier. (2024). <https://doi.org/10.1016/B978-0-12-824315-2.00175-5>
49. Kuo, I. Y. & Ehrlich, B. E. Signaling in muscle contraction. *Cold Spring Harb. Perspect. Biol.* **7** (2), a006023. <https://doi.org/10.1101/cshperspect.a006023> (2015).
50. Khaziev, E. et al. Acetylcholine-Induced Inhibition of Presynaptic Calcium Signals and Transmitter Release in the Frog Neuromuscular Junction. *Front. Physiol.* **7** <https://doi.org/10.3389/fphys.2016.00621> (2016).
51. El-Saeid, M. H. et al. Impact of photolysis and TiO₂ on pesticides degradation in wastewater. *Water* **13**, 655. <https://doi.org/10.3390/w13050655> (2021).
52. Choi, J. & Chung, J. Photodegradation of low molecular weight organic compounds by 185-nm UV light in ultrapure water production system. *J. Water Process. Eng.* **37**, 101437. <https://doi.org/10.1016/j.wpe.2020.101437> (2020).
53. Florêncio, M. H. et al. Photodegradation of Diquat and Paraquat in aqueous solutions by titanium dioxide: evolution of degradation reactions and characterization of intermediates. *Chemosphere* **55** (3), 345–355. <https://doi.org/10.1016/j.chemosphere.2003.11.013> (2004).
54. Müller, K. R. et al. *AnacaMicrocarpumcarpum* extract and fractions protect against paraquat-induced toxicity in *Drosophila melanogaster*. *EXCLI J.* **16**, 302–312. <https://doi.org/10.17179/excli2016-684> (2017).
55. Duavy, S. M. et al. Pequi enriched diets protect *Drosophila melanogaster* against paraquat-induced locomotor deficits and oxidative stress. *J. Toxicol. Environ. Health Part. A*. **82** (11), 664–677. <https://doi.org/10.1080/15287394.2019.1642277> (2019).
56. Liang, X., Yang, H. & Liu, Z. Signaling pathways involved in paraquat-induced pulmonary toxicity: molecular mechanisms and potential therapeutic drugs. *Int. Immunopharmacol.* **113**, 109301. <https://doi.org/10.1016/j.intimp.2022.109301> (2022).
57. Neves, P. F. R. et al. Age-related tolerance to paraquat-induced parkinsonism in *Drosophila melanogaster*. *Toxicol. Lett.* **361**, 43–53. <https://doi.org/10.1016/j.toxlet.2022.03.010> (2022).
58. Blanco-Ayala, T., Andérica-Romero, A. C. & Pedraza-Chaverri, J. New insights into antioxidant strategies against paraquat toxicity. *Free Radic. Res.* **48** (6), 623–640. <https://doi.org/10.3109/10715762.2014.899694> (2014).
59. Medina-Leendertz, S. et al. Longterm melatonin administration alleviates paraquat mediated oxidative stress in *Drosophila melanogaster*. *Invest. Clin.* **55** (4), 352–364 (2014).
60. Cassar, M. et al. A dopamine receptor contributes to paraquat-induced neurotoxicity in *Drosophila*. *Hum. Mol. Genet.* **24** (1), 197–212. <https://doi.org/10.1093/hmg/ddu430> (2015).
61. Zhang, X., Thompson, M. & Xu, Y. Multifactorial theory applied to the neurotoxicity of paraquat and paraquat-induced mechanisms of developing Parkinson's disease. *Lab. Invest.* **96** (5), 496–507. <https://doi.org/10.1038/labinvest.2015.161> (2016).
62. Ahmad, M. H., Fatima, M., Ali, M., Rizvi, M. A. & Mondal, A. C. Naringenin alleviates paraquat-induced dopaminergic neuronal loss in SH-SY5Y cells and a rat model of Parkinson's disease. *Neuropharmacology* **201**, 108831. <https://doi.org/10.1016/j.neuropharm.2021.108831> (2021).
63. Hajam, Y. A. et al. Oxidative stress in Human Pathology and Aging: Molecular mechanisms and perspectives. *Cells* **11** (3), 552. <https://doi.org/10.3390/cells11030552> (2022).
64. Harris, R. A. et al. Aerobic glycolysis in the Frontal Cortex Correlates with memory performance in wild-type mice but not the APP/PS1 mouse model of cerebral amyloidosis. *J. Neurosci.* **36** (6), 1871–1878. <https://doi.org/10.1523/JNEUROSCI.3131-15.2016> (2016).

65. Hosamani, R. Acute exposure of *Drosophila melanogaster* to paraquat causes oxidative stress and mitochondrial dysfunction. *Arch. Insect Biochem. Physiol.* **83** (1), 25–40. <https://doi.org/10.1002/arch.21094> (2013).
66. Jang, Y. J. et al. Paraquat induces apoptosis through a Mitochondria-Dependent pathway in RAW264.7 cells. *Biomolecules Ther.* **23** (5), 407–413. <https://doi.org/10.4062/biomolther.2015.075> (2015).
67. Chowdhury, A. R. et al. Mitochondria-targeted paraquat and metformin mediate ROS production to induce multiple pathways of retrograde signaling: a dose-dependent phenomenon. *Redox Biol.* **36**, 101606. <https://doi.org/10.1016/j.redox.2020.101606> (2020).
68. Carmo, M. K. B., Figueiredo, M. O. V., Souza, J. M., Souza, A. O. & Lima, C. A. C. neuroprotective action of aspirin on Paraquat intoxication in on *Drosophila melanogaster*. *Res. Soc. Dev.* **10** (4), e30710414179. <https://doi.org/10.33448/rsd-v10i4.14179> (2021).
69. Wang, X. H., Souders, C. L., Zhao, Y. H. & Martyniuk, C. J. Paraquat affects mitochondrial bioenergetics, dopamine system expression, and locomotor activity in zebrafish (*Danio rerio*). *Chemosphere* **191**, 106–117. <https://doi.org/10.1016/j.chemosphere.2017.10.032> (2018).
70. Li, W. et al. Oxaloacetate acid ameliorates paraquat-induced acute lung injury by alleviating oxidative stress and mitochondrial dysfunction. *Front. Pharmacol.* **13** <https://doi.org/10.3389/fphar.2022.1029775> (2022).
71. Jones, R. An Acetylcholine Receptor Keeps Muscles in Balance. *PLoS Biol* **7**(12), e1000268. <https://doi.org/10.1371/journal.pbio.1000268> (2009).
72. Seto, Y., Shinohara, T. Structure-activity relationship of reversible cholinesterase inhibitors including paraquat. *Arch Toxicol* **62**, 37–40. <https://doi.org/10.1007/BF0031625> (1988).
73. Aldunate, R., Casar, J. C., Brandan, E., Inestrosa, N. C. Structural and functional organization of synaptic acetylcholinesterase. *Brain Res Brain Res Rev.* **47**(1–3), 96–104. <https://doi.org/10.1016/j.brainresrev.2004.07.019> (2004).
74. de Oliveira Souza, A., Couto-Lima, C. A., Rosa Machado, M. C., Espreafico, E. M., Pinheiro Ramos, R. G., & Alberici, L. C. Protective action of Omega-3 on paraquat intoxication in *Drosophila melanogaster*. *J Toxicology Environ Health Part A* **80**(19–21), 1050–1063. <https://doi.org/10.1080/15287394.2017.1357345> (2017).

Acknowledgements

The authors are grateful to the Federal University of Mato Grosso and the University of Caxias do Sul. They would also like to thank two anonymous reviewers for their support through constructive suggestions and corrections on this manuscript.

Author contributions

D.L.R.; M.F.B.; S.M.; A.O.S. Conception, design, development of the methodology, analysis, and interpretation of data, writing, and revision of the manuscript. J.R.S.; M.E.M.M.S.; M.E.S.S.; A.A.T.J.; T.H.O.A.; Performed investigation. A.O.S. supervised the project. All authors reviewed the manuscript.

Funding

This research received no specific grant from any funding agency in the public, commercial, or not-for-profit sectors.

Declarations

Competing interests

The authors declare no competing interests.

Additional information

Supplementary Information The online version contains supplementary material available at <https://doi.org/10.1038/s41598-025-86413-0>.

Correspondence and requests for materials should be addressed to A.O.S.

Reprints and permissions information is available at www.nature.com/reprints.

Publisher's note Springer Nature remains neutral with regard to jurisdictional claims in published maps and institutional affiliations.

Open Access This article is licensed under a Creative Commons Attribution-NonCommercial-NoDerivatives 4.0 International License, which permits any non-commercial use, sharing, distribution and reproduction in any medium or format, as long as you give appropriate credit to the original author(s) and the source, provide a link to the Creative Commons licence, and indicate if you modified the licensed material. You do not have permission under this licence to share adapted material derived from this article or parts of it. The images or other third party material in this article are included in the article's Creative Commons licence, unless indicated otherwise in a credit line to the material. If material is not included in the article's Creative Commons licence and your intended use is not permitted by statutory regulation or exceeds the permitted use, you will need to obtain permission directly from the copyright holder. To view a copy of this licence, visit <http://creativecommons.org/licenses/by-nc-nd/4.0/>.

© The Author(s) 2025